Hindawi
Geofluids
Volume 2022, Article ID 7360065, 19 pages
https://doi.org/10.1155/2022/7360065

Research Article

Geochemical Characteristics and Organic Matter Accumulation of Wufeng-Longmaxi Shales in the Southeast of the Sichuan Basin of South China

Ying Zhang[1,2] **Chengfu Lyu**[1,3] **Xue Gao**[1,2] **Zhaoqing Dang**[1,2] **Zhaotong Sun**[1,2] **Qianshan Zhou**[1,3] **and Guojun Chen**[1,3]

[1]*Northwest Institute of Eco-Environment and Resources, Chinese Academy of Sciences, Lanzhou 730000, China*
[2]*University of Chinese Academy of Sciences, Beijing 100049, China*
[3]*Key Laboratory of Petroleum Resources, Gansu Province, Lanzhou 730000, China*

Correspondence should be addressed to Chengfu Lyu; chengfu_lyu@126.com

Received 5 September 2022; Revised 28 October 2022; Accepted 8 November 2022; Published 19 December 2022

Academic Editor: Shengnan Nancy Chen

The Upper Ordovician Wufeng Formation and Lower Silurian Longmaxi Formation black shales are the critical targets for shale gas exploration in the Sichuan Basin of South China. The enrichment of organic matter (OM) in shale is the basis for the generation of large-scale shale gas; however, its controlling factors in Wufeng-Longmaxi shales are still under debate, and few studies have focused on the edge of the Sichuan Basin. Based on the mineral composition, total organic carbon (TOC), and systematic inorganic geochemistry analysis of 72 core samples from Wufeng and Longmaxi formations in Well Xike 1, southeastern Sichuan Basin, the sedimentary conditions (palaeoclimate, palaeoredox, and palaeoproductivity) were reconstructed, and the controlling factors of OM enrichment were identified. The mineral compositions are dominated by quartz, clay minerals, calcite, and feldspar, associated with minor dolomite, pyrite, and anhydrite. The TOC contents (0.31%-6.84%, avg. 2.22%) show an upward decreasing trend from the Wufeng Formation to Longmaxi Formation. The chemical index of alteration (CIA) ranges from 65 to 71 (avg. 69), indicating warm and humid climate with moderate weathering. The diagrams of Al_2O_3-TiO_2, TiO_2-Zr, Zr/Sc-Th/Sc, La/Th-Hf, and La-Th-Sc jointly indicate the contribution from felsic and intermediate rock weathering. The P/Al, Cu/Al, and Ni/Al ratios suggest that marine paleoproductivity was relatively high in the Wufeng Formation and relatively low to moderate in the Longmaxi Formation. The V/Cr, V/Sc, U/Th, Mo_{EF}/U_{EF}, and C_{org}/P ratios indicate that the bottom water was anoxic during the Wufeng Formation deposition and then fluctuating dysoxic and/or oxic in the overlying Longmaxi Formation. The TOC content was positively correlated with productivity proxies (P/Al, Cu/Al, and Ni/Al) as well as redox proxies (U/Th, V/Cr, Mo_{EF}/U_{EF}, and C_{org}/P), indicating that the OM accumulation in Wufeng-Longmaxi shales is mainly controlled by high productivity and anoxic bottom water conditions.

1. Introduction

For the past few years, following with the rapid production growth and commercial exploration and development of shale gas in the United States, shale gas gradually attracted worldwide attention and greatly stimulated the enthusiasm of shale gas exploration and development in China [1–4]. Organic-rich marine shales are generally characterized by wide distribution area, diversified lithofacies types, diverse sedimentary environments, and also complicated mechanical properties [5–8]. The recoverable shale gas resources in South China, especially the Sichuan Basin, account for nearly 50% of the total unconventional resources in China [9].

The favorable conditions of shale gas accumulation (e.g., lithology, gas generating conditions, and preservation conditions) in Sichuan Basin of South China is similar to those of eastern basins in the United States, where shale gas exploration is proved to be successful. Unlike conventional reservoirs, the organic matter (OM) in shale is commonly considered as a critical factor for shale gas accumulation

owing to its generation and adsorption carriers for shale gas [10]. The black shales from the Upper Ordovician Wufeng Formation and Lower Silurian Longmaxi Formation are widely distributed in the Sichuan Basin and characterized by high OM contents, moderate maturity, well-developed microfractures, and moderate burial depth [11–14]. Although deposition of OM enrichment shales from Wufeng and Longmaxi Formations has been extensively investigated in Sichuan Basin, the controlling factors for OM enrichment are still under debate. Some authors have suggested that the OM enrichment in Wufeng-Longmaxi samples is closely related to the productivity of OM, that is, to the primary production [15], whereas others have proved that the OM enrichment depends on its preservation conditions; that is, it is related to the anoxic bottom water conditions [16–18]. Besides, the geological events (e.g., volcanic activity and glacial period) may also play a crucial role in OM enrichment owing to anoxic water conditions and/or weathering input of nutrient caused by volcanism [19]. Thus, more work are required to carefully explore the mechanisms of OM accumulation in Wufeng-Longmaxi shales.

The migration, accumulation, and distribution of redox-sensitive elements in sedimentary rocks record the information of changes in sedimentary paleoenvironment [20, 21]. Previous studies have shown that redox-sensitive elements are obviously controlled by redox conditions of bottom waters and generally become enriched under more reducing waters [22, 23]. Therefore, trace redox changes in bottom waters (e.g., oxic, dyoxic, and anoxic) are mainly indicated by changes in ratios of redox-sensitive elements and their enrichment factors in the sediment. The enrichment factor of trace elements is expressed as $EF_{element}\ X = (X/Al)_{sample/}(X/Al)_{average\ shale}$ [24], and the average shale refers to the average Post-Archean Australian Shale (PAAS) [25]. The nutrient elements (e.g., P and Cu) are essential for living organism, and their enrichment in the water column stimulates marine productivity [15]. Therefore, high level of nutrient elemental contents in marine sediments may suggest high marine productivity. To dilute the influence of terrigenous detrital, their concentrations relative to Al contents (e.g., P/Al, Cu/Al, and Ni/Al) are used to trace the changes in productivity. The CIA index is commonly used to evaluate the degree of chemical weathering and changes in paleoclimate [19, 26]. Other ratios of trace elements (e.g., TiO_2-Zr, Th/Sc-Zr/Sc, and La/Th-Hf) are used to trace the sources of marine sediments, classifying them as mafic, intermediate, basic, and felsic igneous [27–30].

Many studies have focused on the sedimentary environment and OM enrichment of Wufeng Formation and Longmaxi Formation shales in the inner regions of Sichuan Basin, but few studies have focused on the edge of the Sichuan Basin. Here, we collected complete succession of Wufeng-Longmaxi shale core samples from Xike 1 well in the southeast margin of Sichuan Basin to reconstruct the depositional paleoenvironment (palaeoclimate, primary productivity, and redox conditions) and explore the mechanisms of OM accumulation. Our study could provide the geological theoretical basis for the exploration and development of Upper Ordovician-Lower Silurian shale gas in southeastern Sichuan Basin.

2. Geological Setting

Sichuan Basin, located in the northwest of the Yangtze Block in South China, is a compressional tectonic basin undergoing multiple thrust nappe structures in Mesozoic era [31], consisting mainly of marine and continental facies [11, 32]. The margin of the basin is surrounded by orogenic belts, including Micang Mountain in the north, Daba Mountain in the northeast, Longmen Mountain in the northwest, Dalou Mountain in the south, and Jiangnan-Xuefeng Mountain in the southeast [33]. The basement of Sichuan Basin is composed of a suite of Sinian magmatic rocks and metamorphic rocks [34, 35]. The sedimentary black shale successions include six units in Sichuan Basin (Middle and Lower Jurassic, Upper Triassic, Permian, Lower Silurian, Upper Ordovician, and Lower Cambrian) [31, 36]. The Upper Ordovician-Lower Silurian Wufeng-Longmaxi shales are the important shale gas targets and also the main contribution of shale gas exploration and development in Sichuan Basin [37].

Our studied drillcore (Xike 1) is located in the transitional zone between northern Guizhou and southeastern Sichuan ([38, 39], Figure 1). In the Late Ordovician, widespread anoxic sedimentary environment with weak hydrodynamic force was developed following with the Guangxi movement and resultant paleouplift of central Sichuan, central Guizhou, and Xuefengshan [40]. The Wufeng-Longmaxi Formation of the Late Ordovician-Early Silurian was well developed in our studied area, while they are missing in most areas of southern Guizhou owing to the influence of the Middle Guizhou uplift [41]. The Upper Ordovician-Lower Silurian OM enrichment shales are mainly deposited in the shallow-deep water shelf facies with variable thickness [42]. Influenced by the Qiyueshan fault, the fault system in the core of Xishui anticline is relatively developed [43]. The drillcore Xike 1 covers four formations: Longmaxi Formation, Guanyinqiao Formation, Wufeng Formation and Jiancaogou Formation. The Longmaxi Formation is subdivided into Upper Longmaxi Formation and Lower Longmaxi Formation, from top to bottom, including Silurian Upper Longmaxi Formation (2.16-69.76 m), Lower Longmaxi Formation (69.76-136.10 m), Upper Ordovician Guanyinqiao Formation (136.10-136.80 m), Upper Ordovician Wufeng Formation (136.80-143.84 m), and Jiancaogou Formation (143.84-149.36 m). The core samples covering Wufeng Formation and Longmaxi Formation from XK1 well are the main target of this study. The thickness of Longmaxi Formation is 133.94 m, and the thickness of Wufeng Formation is 7.04 m, dominated by the black shale.

3. Material and Methods

A total of 72 core samples covering Wufeng-Longmaxi Formation were collected from Xike 1 well for geochemical analysis. Before analysis, all the samples were grind to 200 mesh and dried at 105°C for 4 h. The 80 mesh powered samples are required for total organic carbon analysis.

The minerals compositions were determined by X-ray diffraction (XRD) methods using Rigaku Ultima IV (Japan), with the accuracy of 1.0%. The detailed processes are as

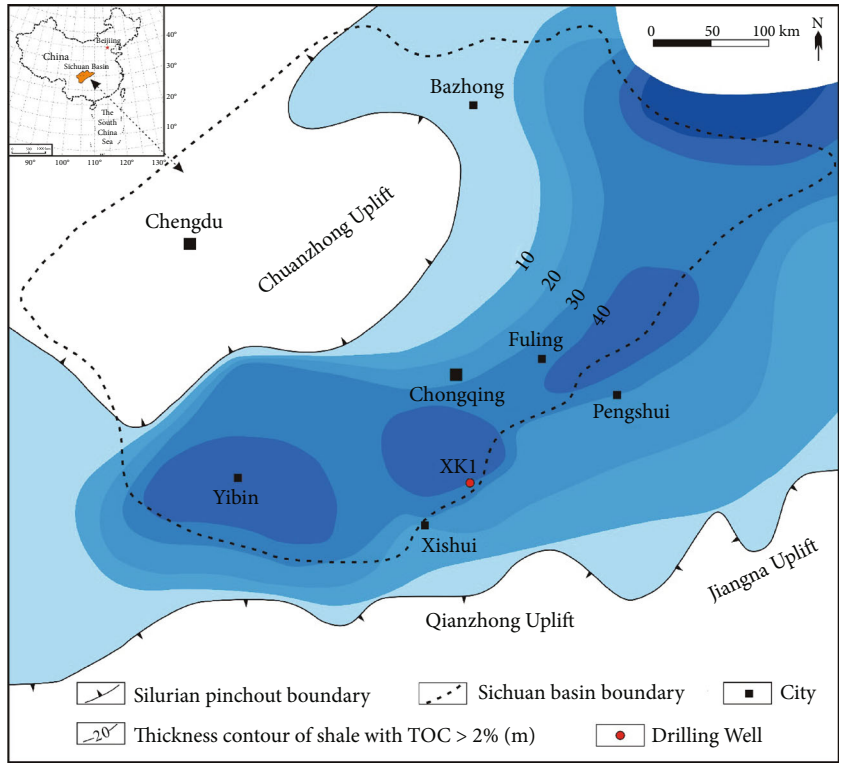

Figure 1: The location map of sampling in the study area of Sichuan Basin [71].

follows: (1) X-ray generator (3 kW, Cu Kα), (2) goniometer (285 mm) with goniometer range of -110~180°, and (3) detector: one-dimensional high-speed omnipotent matrix detector with active area of 12.8×20 mm, maximum count with 1×10^{12} cps. The scanning speed is 3°/min, and the scanning angle is in the range of 3°–50°. Generally, the accuracy and stability of test samples are better than ±0.02° and ±0.002 in this study, respectively.

Major element experiments were conducted by a fully automated sequential wavelength dispersive X-ray fluorescence spectrometry with Axios, Super Sharp Tube of Rh-anode, and analysis software SuperQ Version 5. The test conditions were 4.0 kW, 60 kV, and 160 mA. The sample for XRF experiment was treated as follows: the 4 g sample was crushed to less than 200 mesh, dried at 105°C, and then put into the sample preparation mold to complete sample preparation. The accuracy of standard and duplicate samples is generally better than 2.0%.

Trace elements were measured by inductively coupled plasma mass spectrometry (ICP-MS; Agilent 7700e). Before analysis, about 50.00 mg of powered samples was firstly dissolved using 1.50 ml nitric acid (HNO_3), 1.50 ml hydrofluoric acid (HF), and 0.01 ml perchloric acid ($HClO_4$) in a sealed container. The sealed container was placed on a heating plate and evaporated to near dryness at 140°C. Then, 1.50 ml of HNO_3 and 1.50 ml of HF were added to the container and mixed with the sample and heated in an oven at 195 ± 5°C for 48 h to better digest powered samples, and acid solution was evaporated on a heating plate until nearly dry. The dried residue was mixed with 2.0 ml HNO_3 and dried again, and this process was repeated. Then, 3 ml of HNO_3 with a volume fraction of 50% was added to the sample and placed in a sealed container for heating for 3 h and cooling. Finally, the residue solution was diluted to 50 ml using ultrapure water for ICP-MS analysis. The accuracy of standard and duplicate samples is generally better than 2.0%.

Total organic carbon (TOC) content was performed using the LECO CS-344 carbon and sulfur analyzer. About 0.1 g of 80 mesh powered samples was taken to completely eliminate the carbonate with 5% hydrochloric acid (HCl), and then the residue was washed with distilled water. After treatment, it was then preserved and dried in an oven at 40-60°C for 12 h. The sensitivity of instrument and the accuracy of standard and duplicate samples are generally better than 0.1 μg/g and 0.1%, respectively.

All the above experiments (XRD, XRF, ICP-MS, and TOC) were conducted at Oil and Gas Research Center, Northwest Institute of Eco-Environment and Resources, Chinese Academy of Science (CAS).

4. Results

4.1. Minerals and TOC Contents. XRD results show that quartz, clay minerals, calcite, and feldspar are the main minerals in Wufeng Formation and Longmaxi Formation, while dolomite, pyrite, and anhydrite are the minority minerals (Figure 2). The main mineral compositions for Xike 1 (XK1) well are as follows: quartz (10.3%~75.8%, with an average of 47.6%), clay minerals (4.3%~45.1%, with an average of 26.1%), calcite (1.1%~82.8%, with an average of 9.1%), feldspar

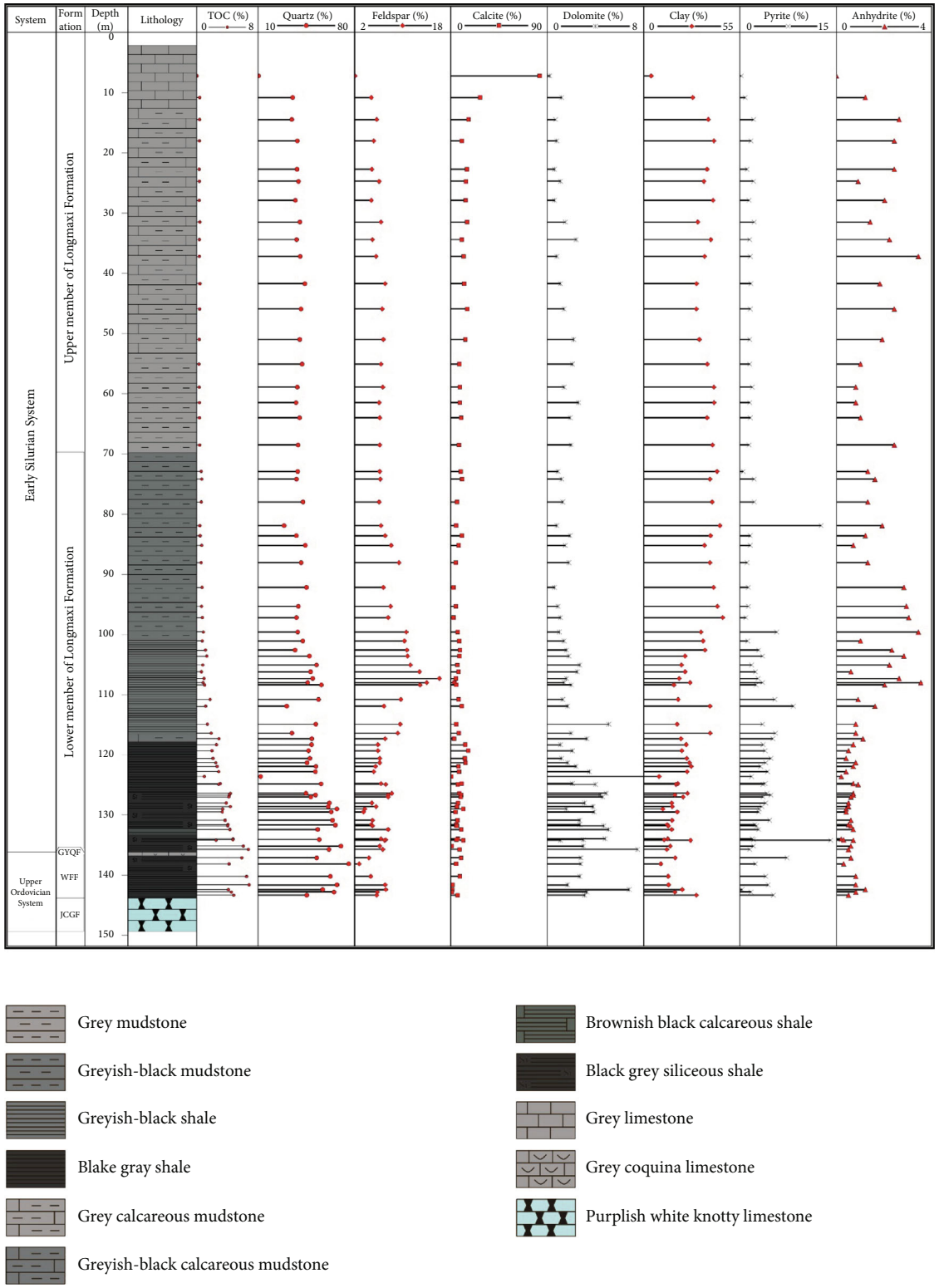

Figure 2: Vertical lithology variations of studied sample from XK1 well (GYQF: Guanyinqiao Formation; WFF: Wufeng Formation; JCGF: Jiancaogou Formation).

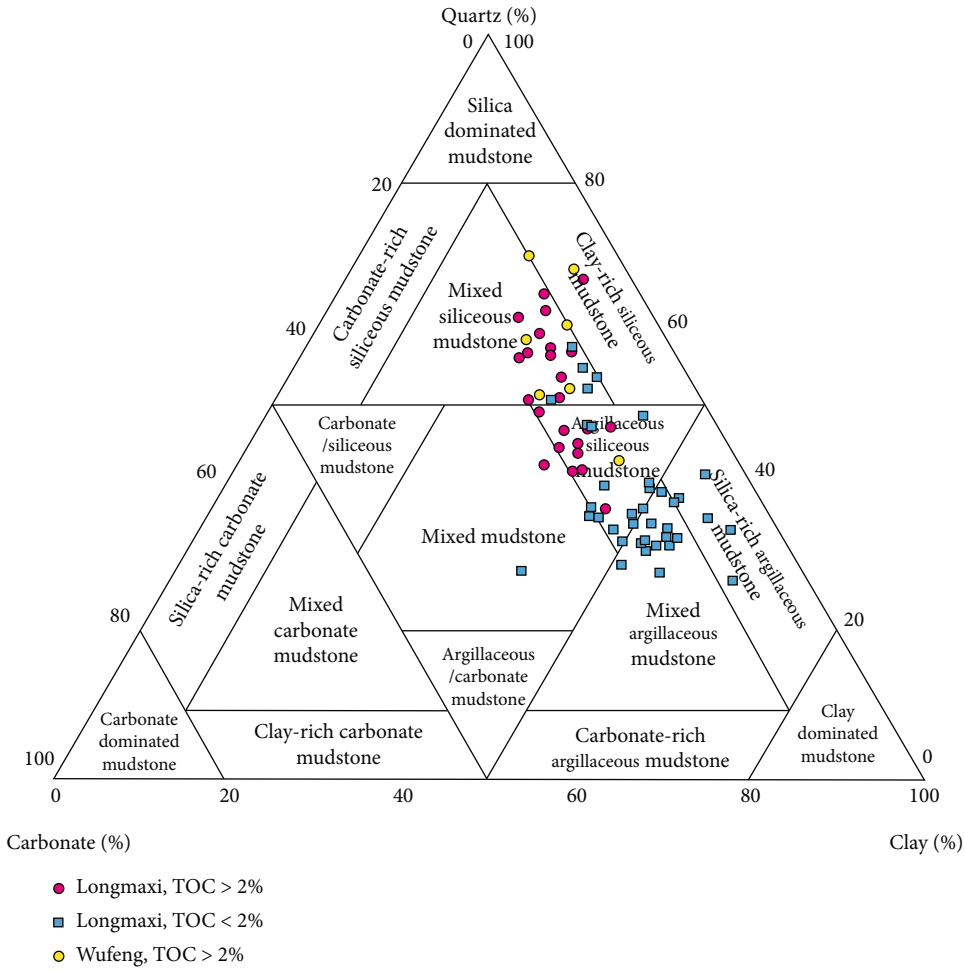

Figure 3: The terminology and classification of black shale from XK1 well.

(1.4%~16.1%, with an average of 6.9%), dolomite (0.3%~75.6%, with an average of 5.5%), pyrite (0.2%~14.1%, with an average of 3.1%), and anhydrite (0.2%~3.5%, with an average of 1.2%). TOC contents range from 0.09% to 6.84% and show a decreasing trend from Wufeng Formation to Longmaxi Formation. As shown in Figure 3, mixed argillaceous mudstone, argillaceous/siliceous mudstone, and mixed siliceous mudstone are mainly identified in our studied samples.

4.2. Major Element Geochemistry. According to XRF data, the major elements are mainly SiO_2 and Al_2O_3 in the samples from Wufeng Formation and Longmaxi Formation (Table 1). SiO_2 contents range from 15.10% to 73.49% (avg. 57.50%). Then, the content of Al_2O_3, Fe_2O_3, MgO, and K_2O varies from 4.43% to 21.52% (avg. 15.87%), 1.75% to 8.11% (avg. 4.90%), 0.98% to 11.25% (avg. 3.27%), and 1.01% to 5.29% (avg. 3.65%), respectively. The CaO contents are relatively high variables (1.83%~50.14%, avg. 6.49%). Other major element oxide (Na_2O, P_2O_5, and TiO_2) contents are relatively low with an average of 0.89%, 0.10%, and 0.72%, respectively. The Al_2O_3 versus SiO_2 and TiO_2 diagrams of Wufeng and Longmaxi Formation core samples from XK1 well are presented in Figure 4.

4.3. Trace Element Geochemistry. The results of ICP-MS experiment show that the trace elements of samples from XK1 well are listed in Table S1. The average values of Ba (avg. 351.4 ppm) and V (avg. 116.4 ppm), followed by Sr (88.3 ppm), Rb (81.6 ppm), Zr (71 ppm), B (55 ppm), Ce (37 ppm), Cr (36 ppm), Ni (36.5 ppm), and Cu (26 ppm), are relatively abundant in our samples, whereas other elements show lower concentrations with an average of less than 20 ppm, including Sc (5.7 ppm), Co (7.9 ppm), Hf (2.0 ppm), Th (8.1 ppm), and U (5.8 ppm). In this study, the contents of trace elements which can reflect the sedimentary environment are different between Wufeng Formation and Longmaxi Formation. Trace elements reflecting the provenance include Zr, Hf, Th, Sc, and La, whose contents in Wufeng Formation are 23.9-194.8 ppm (avg. 71.2 ppm), 0.6-5.3 ppm (avg. 2.1 ppm), 4.1-21.4 ppm (avg. 8.5 ppm), 2.1-8.7 ppm (avg. 6.0 ppm), and 9.5-28.2 ppm (avg. 19.7 ppm), respectively. In Longmaxi Formation, its contents are 32.2-108.5 ppm (avg. 76.3 ppm), 0.9-2.6 ppm (avg. 1.7 ppm), 3.4-8.0 ppm (avg. 6.1 ppm), 2.4-6.2 ppm (avg. 4.5 ppm), and 10.1-28.0 ppm (avg. 17.9 ppm), respectively. The contents of trace elements V, Cr, U, and Mo which can reflect the redox conditions in Wufeng

Table 1: Major element concentration and TOC content of the Wufeng and Longmaxi shales.

Formation	Sample	SiO_2/%	Al_2O_3/%	CaO/%	K_2O/%	Na_2O/%	MgO/%	Fe_2O_3/%	P_2O_5/%	TiO_2/%	TOC/%	CIA
Longmaxi Formation	XK1-3	44.18	14.99	18.57	3.57	0.49	3.80	4.92	0.07	0.88	0.41	73
	XK1-6	52.82	18.66	7.03	4.40	0.66	4.57	6.24	0.08	0.85	0.38	73
	XK1-8	51.46	18.15	8.37	4.28	0.77	4.45	6.08	0.08	0.88	0.34	72
	XK1-12	52.23	18.13	7.84	4.22	0.82	4.41	6.20	0.08	0.87	0.34	71
	XK1-15	51.34	17.81	8.81	4.14	0.86	4.34	5.91	0.08	0.90	0.44	71
	XK1-16	52.95	18.23	7.38	4.24	0.82	4.41	6.12	0.08	0.86	0.37	71
	XK1-17	48.30	18.31	7.36	4.16	0.85	4.45	6.26	0.07	0.82	0.36	71
	XK1-18	53.14	18.43	7.36	4.26	0.95	4.19	5.66	0.09	0.89	0.45	70
	XK1-21	52.16	18.22	7.45	4.25	0.74	4.47	6.30	0.08	0.86	0.40	72
	XK1-23	51.88	16.85	9.91	3.70	1.03	3.94	5.52	0.09	0.87	0.34	69
	XK1-25	55.48	18.71	5.06	4.30	1.04	4.38	6.26	0.08	0.80	0.31	70
	XK1-26	54.38	18.47	5.91	4.15	1.01	4.45	6.35	0.08	0.85	0.34	70
	XK1-27	54.79	18.38	5.49	4.17	0.99	4.41	6.34	0.08	0.82	0.38	70
	XK1-28	53.89	18.44	6.40	4.24	1.01	4.50	6.24	0.09	0.84	0.38	70
	XK1-30	55.88	18.86	4.13	4.30	0.89	4.43	6.50	0.08	0.80	0.42	71
	XK1-32	55.27	18.32	4.87	4.11	0.90	4.37	6.26	0.08	0.85	0.60	71
	XK1-33	54.74	18.24	5.90	4.14	0.91	4.25	6.18	0.09	0.86	0.67	71
	XK1-34	57.71	19.09	2.88	4.36	0.96	4.31	6.30	0.08	0.76	0.61	71
	XK1-35	51.84	21.52	2.48	4.73	0.86	4.13	9.26	0.07	1.50	0.44	73
	XK1-38	57.78	19.02	2.96	4.33	0.95	4.21	6.08	0.09	0.76	0.66	71
	XK1-40	56.69	19.25	3.06	4.37	0.95	4.39	6.47	0.10	0.77	0.59	71
	XK1-43	58.09	19.94	1.83	4.66	0.95	4.42	6.43	0.09	0.73	0.71	71
	XK1-45	57.79	19.92	2.38	4.68	0.89	4.42	6.20	0.09	0.73	0.64	71
	XK1-47	57.28	20.09	2.14	4.70	0.95	4.44	6.25	0.08	0.73	0.76	71
	XK1-49	56.42	19.49	3.26	4.38	1.12	4.19	6.28	0.10	0.76	0.88	70
	XK1-50	57.05	18.96	3.80	4.23	1.19	4.01	5.42	0.10	0.79	0.74	69
	XK1-51	54.96	22.37	3.45	5.04	1.00	4.10	5.41	0.11	0.66	1.17	72
	XK1-52	56.42	18.77	3.84	4.20	1.26	3.82	5.53	0.10	0.79	1.33	68
	XK1-53	57.16	17.92	4.34	3.83	1.45	3.79	4.87	0.11	0.78	0.81	67
	XK1-54	54.57	19.09	5.13	3.98	1.39	3.92	5.37	0.11	0.75	0.63	68
	XK1-55	57.27	17.27	4.70	3.62	1.44	3.49	4.80	0.11	0.82	0.97	67
	XK1-56	56.73	19.91	3.03	4.21	1.35	3.73	5.59	0.12	0.74	0.85	69
	XK1-57	57.58	16.94	4.51	3.51	1.49	3.37	4.78	0.11	0.80	1.05	66
	XK1-58	58.48	18.30	3.81	4.13	1.08	3.41	5.03	0.11	0.82	1.77	69
	XK1-59	54.60	23.44	3.28	5.34	0.93	4.02	5.91	0.07	0.82	1.19	73
	XK1-60	58.36	15.53	5.11	3.38	1.18	3.20	5.01	0.12	0.75	1.42	67
	XK1-61	56.42	23.50	2.98	5.29	1.07	3.74	4.80	0.10	0.55	1.90	72
	XK1-62	58.65	17.00	4.89	4.04	0.88	3.55	4.87	0.15	0.78	2.91	70
	XK1-63	59.84	15.90	5.96	3.84	0.77	2.57	4.38	0.12	0.75	2.59	70
	XK1-64	56.52	16.23	8.22	3.82	0.81	2.77	4.71	0.11	0.75	2.00	70
	XK1-65	60.11	14.61	7.04	3.47	0.74	2.56	4.23	0.10	0.67	2.14	70
	XK1-66	58.71	16.16	6.09	3.82	0.80	2.75	4.69	0.11	0.69	2.50	70
	XK1-67	60.39	14.07	6.97	3.32	0.81	2.35	4.17	0.11	0.72	2.67	69
	XK1-68	57.98	14.78	7.55	3.53	0.79	2.67	4.42	0.12	0.76	2.88	70
	XK1-69	19.36	7.69	35.16	1.81	0.40	11.25	8.11	0.08	0.56	1.01	70
	XK1-70	61.65	14.56	5.70	3.46	0.89	2.30	4.04	0.10	0.68	3.09	69
	XK1-71	60.97	14.44	6.33	3.44	0.88	2.42	3.97	0.10	0.68	2.88	69
	XK1-72	57.12	16.36	5.89	3.95	0.96	3.10	4.48	0.11	0.71	4.41	69

Table 1: Continued.

Formation	Sample	SiO_2/%	Al_2O_3/%	CaO/%	K_2O/%	Na_2O/%	MgO/%	Fe_2O_3/%	P_2O_5/%	TiO_2/%	TOC/%	CIA
	XK1-73	60.65	14.50	5.52	3.43	0.85	2.36	4.26	0.12	0.68	4.26	69
	XK1-74	57.98	15.38	6.23	3.65	0.94	2.80	4.45	0.11	0.71	4.20	69
	XK1-75	66.77	11.57	5.05	2.72	0.80	1.65	3.27	0.11	0.56	3.86	67
	XK1-76	67.16	11.74	4.40	2.75	0.77	1.70	3.15	0.11	0.57	4.40	68
	XK1-77	67.88	8.91	8.32	2.03	0.64	1.12	2.62	0.11	0.49	3.40	67
	XK1-78	70.98	9.26	4.81	2.14	0.63	1.23	2.55	0.10	0.44	3.36	68
	XK1-79	66.30	10.57	5.49	2.46	0.74	1.56	3.61	0.11	0.52	3.73	67
	XK1-80	68.67	9.70	4.35	2.22	0.66	1.34	3.05	0.10	0.41	4.09	68
	XK1-81	67.46	10.33	5.51	2.40	0.74	1.52	3.19	0.12	0.51	4.06	67
	XK1-82	60.38	12.71	7.27	3.01	0.90	2.31	3.65	0.11	0.66	4.34	67
	XK1-83	62.94	10.07	8.22	2.40	0.84	1.78	2.94	0.09	0.58	4.76	65
	XK1-84	68.78	9.28	5.13	2.17	0.75	1.17	2.77	0.10	0.51	4.73	66
	XK1-85	57.08	19.28	4.22	4.37	0.95	3.01	6.30	0.08	0.60	2.53	71
	XK1-86	73.49	8.81	2.04	2.04	0.71	1.00	2.49	0.13	0.45	6.10	66
Wufeng Formation	XK1-87	64.55	10.06	5.99	2.32	0.90	1.69	2.75	0.18	0.59	6.75	65
	XK1-88	58.33	8.80	9.93	2.16	0.57	1.44	5.45	0.14	0.52	5.88	68
	XK1-89	74.12	6.19	4.77	1.41	0.55	0.68	2.17	0.08	0.32	4.23	65
	XK1-90	62.73	12.28	6.12	2.95	0.73	1.82	3.43	0.10	0.60	6.51	69
	XK1-91	61.79	17.60	3.09	4.34	0.86	3.16	3.42	0.10	0.80	6.84	70
	XK1-92	65.13	13.62	2.36	3.31	0.79	2.00	3.70	0.11	0.63	4.14	69
	XK1-93	67.20	14.52	2.40	3.41	0.79	2.09	2.89	0.11	0.62	4.53	70
	XK1-94	58.89	17.91	2.81	4.22	0.73	2.45	5.09	0.09	0.81	4.83	72

Formation are 61.7-694.9 ppm (avg. 333.6 ppm), 15.0-58.0 ppm (avg. 41.6 ppm), 2.4-31.2 ppm (avg. 12.8 ppm), and 1.0-67.4 ppm (avg. 39.1 ppm), respectively. In Longmaxi Formation, its contents are 37.9-333.6 ppm (avg. 90.1 ppm), 13.9-53.3 ppm (avg. 36.7 ppm), 1.4-19.5 ppm (avg. 5.0 ppm), and 0.9-49.9 ppm (avg. 11.9 ppm), respectively. The contents of trace elements Cu and Ni, which reflect paleoproductivity, are 30.0-83.8 ppm (avg. 58.5 ppm) and 26.5-104.2 ppm (avg. 61.8 ppm) in Wufeng Formation, respectively. The contents in Longmaxi Formation were 9.4-60.0 ppm (avg. 22.6 ppm) and 14.5-74.4 ppm (avg. 33.7 ppm), respectively.

The total rare element contents (ΣREE) of the Wufeng and Longmaxi shales range from 79.68 ppm to 111.9 ppm (avg. 88.66 ppm) and from 47.863 to 123.9 ppm (avg. 80.93 ppm), respectively (Figure 5), which are lower than the upper continental crust (146.4 ppm) and the North American shales (NASC; 167.41 ppm) [25]. The total light REE (La-Eu, ΣLREE) and total heavy REE (Gd-Lu, ΣHREE) contents range from 39.20 ppm to 115.87 ppm (avg. 79.30 ppm) and 5.62 ppm to 13.40 ppm (avg. 8.23 ppm), respectively. The ratios of ΣLREE and ΣHREE reflect the light-heavy REE fractionation degree, and they vary from 5.59 to 12.51 (avg. 9.7), higher than those of NASC (avg. 7.5) [25], likely suggesting higher enrichment of LREE in the Wufeng and Longmaxi shale. The REE distribution pattern relative to chondrite standard and NASC standard is presented in Figure 6. When normalized to chondrite standard, the slope of La-Eu part (LREE) is higher than that of Gd–Lu part (HREE), indicating a higher LREE enrichment (Figure 6(a)). The REE distribution curves standardized by NASC are relatively flat and parallel (Figure 6(b)). The $(La/Yb)_N$ calculated by NASC standard ranges from 0.95 to 2.01, with an average of 1.52, manifesting that LREE is relatively enriched in our study area. δEu ($\delta Eu = Eu_N/Eu_N^*$) and δCe ($\delta Ce = Ce_N/Ce_N^*$) quantify the decoupling relationship between Eu and Ce and other rare earth elements, respectively, resulting in positive or negative anomalies of Eu and Ce in REE distribution patterns. δEu is a negative anomaly with a range of 0.56~1.05 (avg. 0.91). δCe shows a slight negative anomaly with a range of 0.87~1.05 (avg. 0.99).

5. Discussion

5.1. The Weathering of Igneous Rocks under Warm Climate. The chemical index of alteration (CIA) could reflect the weathering degree of sediment provenance ($CIA = Al_2O_3/(Al_2O_3 + CaO^* + NaO + K_2O) \times 100$, [26]). The CIA values ranged from 50 to 65, representing low weathering rate under a cold and arid climate, while higher values of 65~75 suggest moderate weathering rate in a relatively warm climate. The high level of CIA values (>75) may indicate high weathering rate under a hot and humid climate [26, 44]. In this study, the CIA values ranged from 65 to 71 (avg. 68) in Wufeng Formation and 65 to 72 (avg. 70) in Longmaxi Formation (Table 1, Figure 7), respectively, indicating a typical warm climate with moderate physical

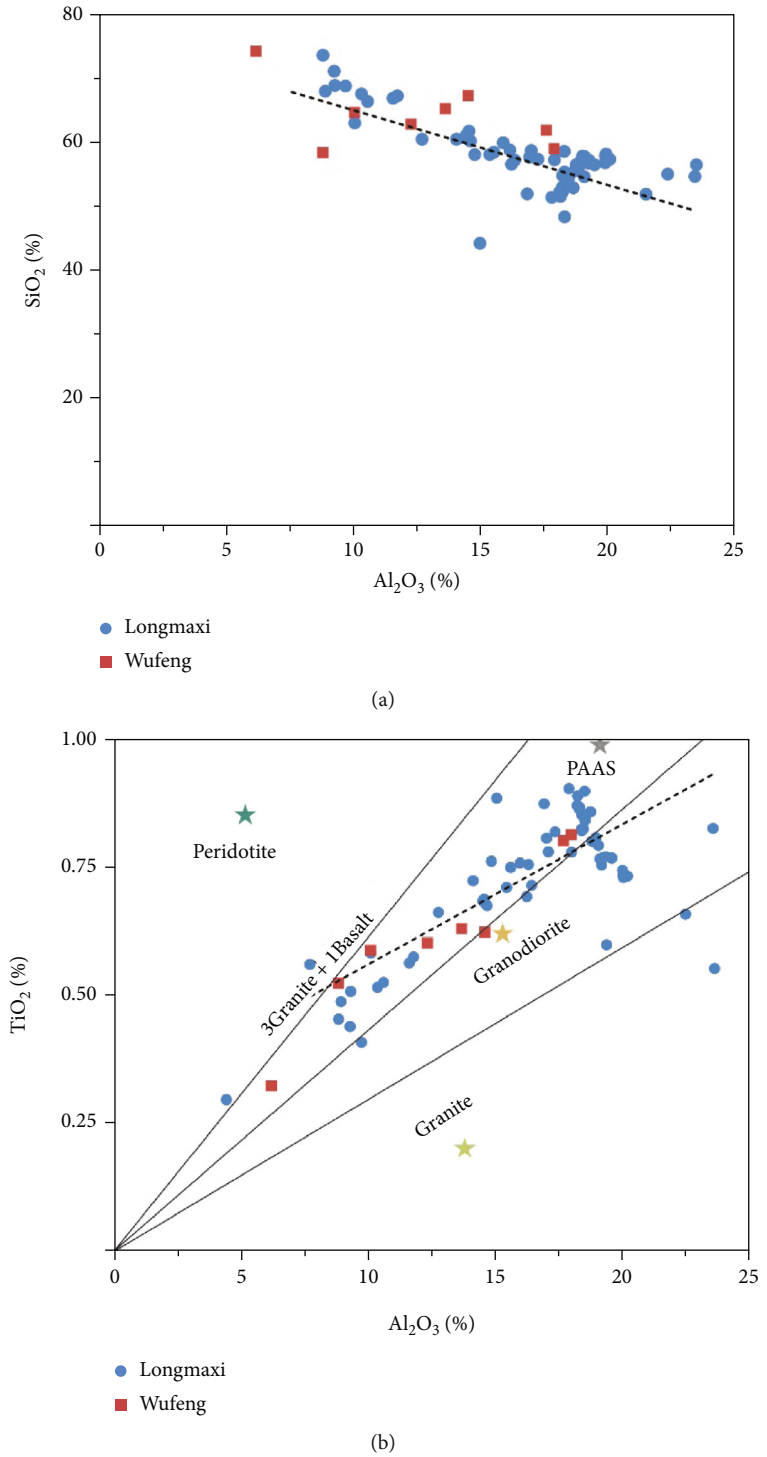

FIGURE 4: (a) SiO_2 versus Al_2O_3 diagram of Wufeng and Longmaxi shales. (b) TiO_2 versus Al_2O_3 diagram of Wufeng and Longmaxi shales; peridotite and granite are representative minerals of ultrabasic and acidic magmatic rocks, respectively; PAAS: average Post-Archean Australian Shale [25, 72, 73].

and chemical weathering during the deposition of Wufeng-Longmaxi Formations samples, and the climate of Longmaxi Formation deposition was warmer than that of Wufeng Formation (Figure 7).

Since aluminum (Al) and titanium (Ti) are not converted and immobile during diagenesis, these two elements are often used as proxies for detrital inputs [16, 24, 45]. In this study, the Al and Ti contents of Wufeng Formation samples range from 3.28% to 9.48% (avg. 6.68%) and 0.19% to 0.49% (avg. 0.37%), respectively. In addition, the Al and Ti contents of Longmaxi Formation samples range from 4.66% to 12.44% (avg. 8.70%) and 0.24% to 0.54%

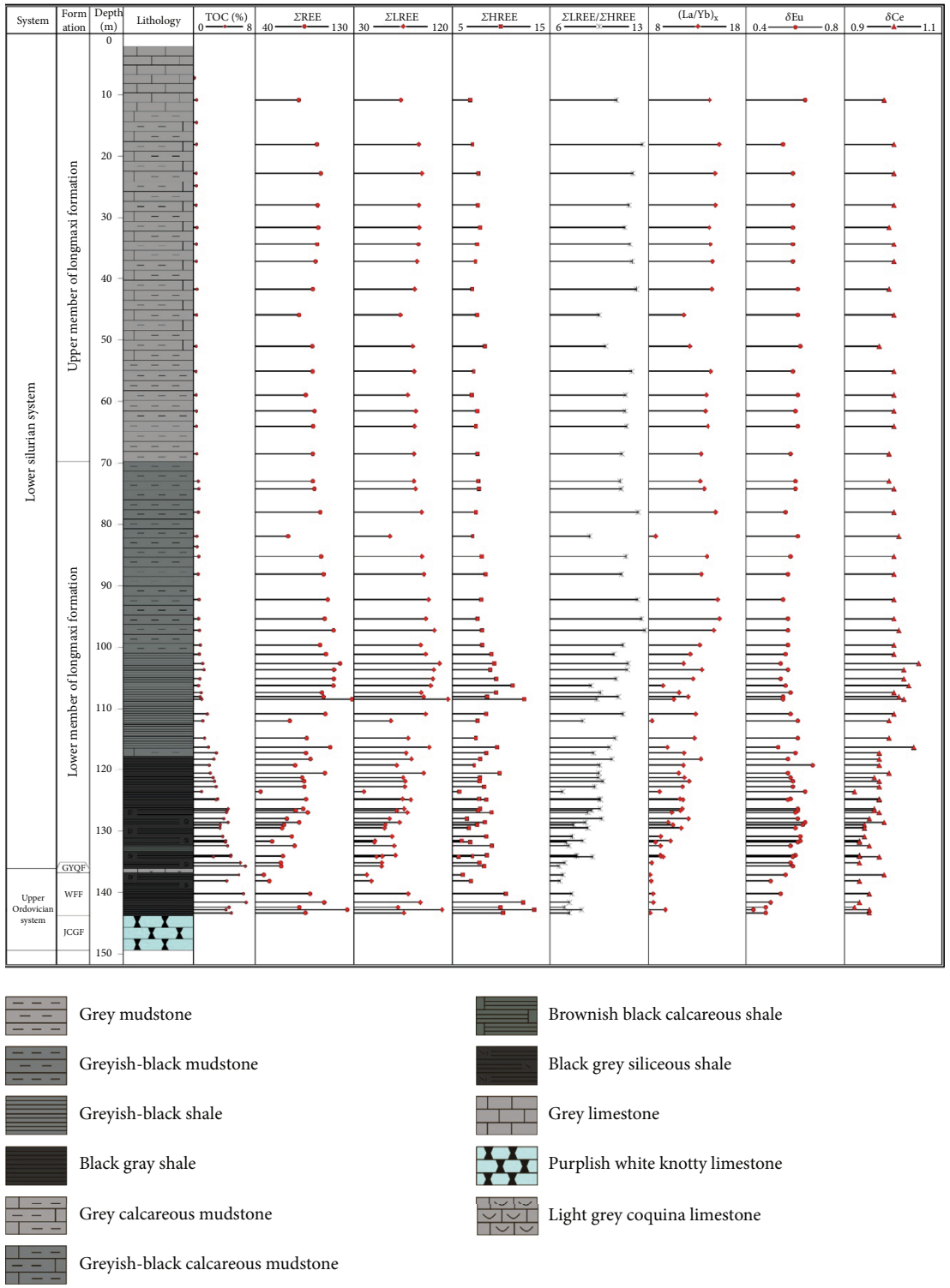

Figure 5: Representative REE parameters of the Wufeng and Longmaxi shales from XK1well (GYQF: Guanyinqiao Formation; WFF: Wufeng Formation; JCGF: Jiancaogou Formation).

(avg. 0.44%), respectively. The proxies of Al and Ti show moderate and lower terrigenous input and less terrigenous input in Wufeng Formation than in Longmaxi Formation (Figure 7).

The diagram of TiO_2 and Al_2O_3 (Figure 4(b)) indicates that the Wufeng-Longmaxi samples are mainly sourced from the weathering of granodiorite, associated with small amount of granite. The range of TiO_2/Zr ratios is also used to identify the weathering sources of marine sediments. The TiO_2/Zr ratios of >200, 199~55, and <55 represent the weathering source of mafic rock, intermediate rock, and felsic igneous, respectively. As shown in Figure 8(a), the TiO_2/

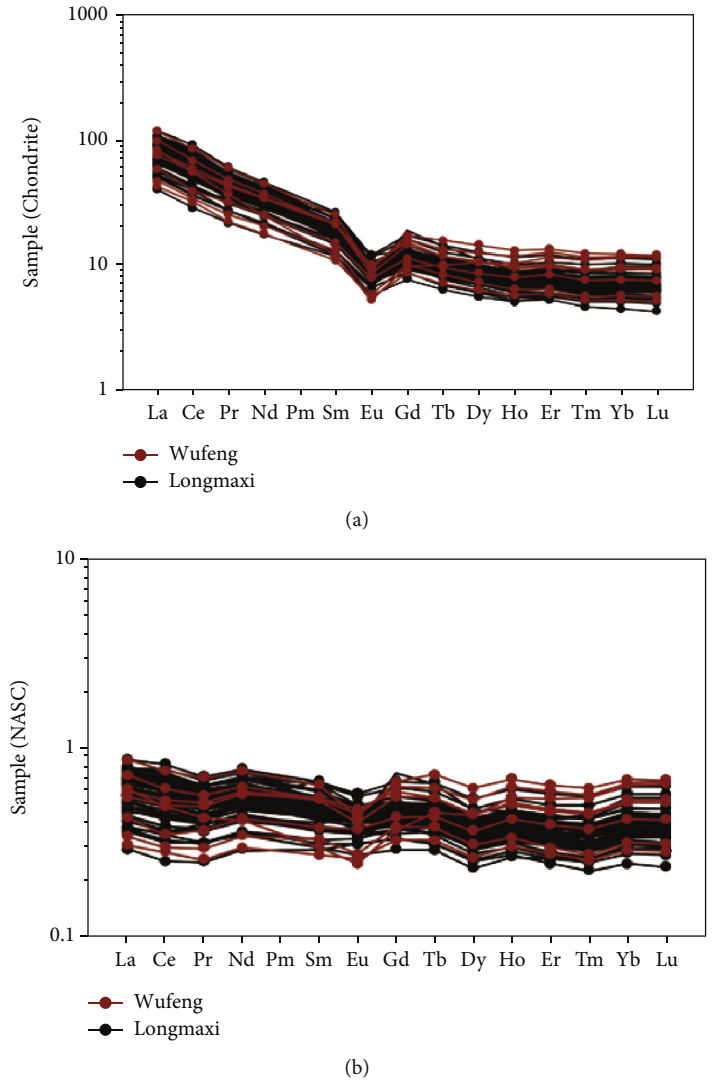

Figure 6: The REE in Wufeng and Longmaxi Formation distribution patterns with chondrite and NASC standard [25].

Zr ratios of the Wufeng and Longmaxi Formation samples range from 39.1 to 199.5 (avg. 120) and 57.8 to 162 (avg. 88.1), respectively, and most of the samples are plotted into the source of intermediate igneous rock regions, while a small part of the samples are plotted into the source of mafic igneous rock and felsic igneous rock. The ratios of the Th/Sc-Zr/Sc are other reliable provenance indicators, and the ratios of La/Th-Hf (Figure 8(b)) and Th/Sc-Zr/Sc (Figure 8(c)) indicate that the provenance rock is more felsic-basic sources, which are also consistent with a granodiorite source (Figure 8(d)). As discussed above, the geochemical indictors showed that the Wufeng and Longmaxi studied samples in XK1well are principally derived from intermediate igneous rocks, accompanied by a small amount of felsic igneous rocks that is similar to granodiorite.

5.2. Fluctuating Anoxic or Dysoxic Bottom Water Conditions. Paleoredox conditions may be closely related to the preservation of OM and enrichment of some trace element in black shales. The contents and existing forms of redox-sensitive trace elements (V, Ni, Co, U, and Mo) transform when the underlying water is changed, and they commonly become enriched in the anoxic water column and are finally preserved in marine sediments under a more reducing environment [24, 46]. In oxic waters, the vanadium (V) exists stably in the form of hydrogen vanadate, which is easily adsorbed by iron/manganese hydroxides or adsorbed by kaolinite [47]. Under weak reduction conditions, the vanadium is reduced from V^{5+} to V^{4+} in the form of vanadium acyl, hydroxyl group, and insoluble hydroxide, which are more likely absorbed by organometallic ligands or by group surface adsorption in the presence of humic and fulic acids and transferred into the sediment [48]. Under a reducing environment, the vanadium (V^{4+}) can be converted to V^{3+} and could be rapidly captured by surrounding porphyrins or precipitated as oxide or hydroxide [49]. Unlike insoluble and nonredox-sensitive thorium (Th), the uranium (U^{6+}) can be reduced to U^{4+} under reduction conditions and then transferred into sediments in the forms of pitchblende or hydroxyl complex with high surface activity [50, 51]. In fulic acid, the processes of uranium organometallic ligands, OM uranium uptake, and bacterial sulfate reduction promote

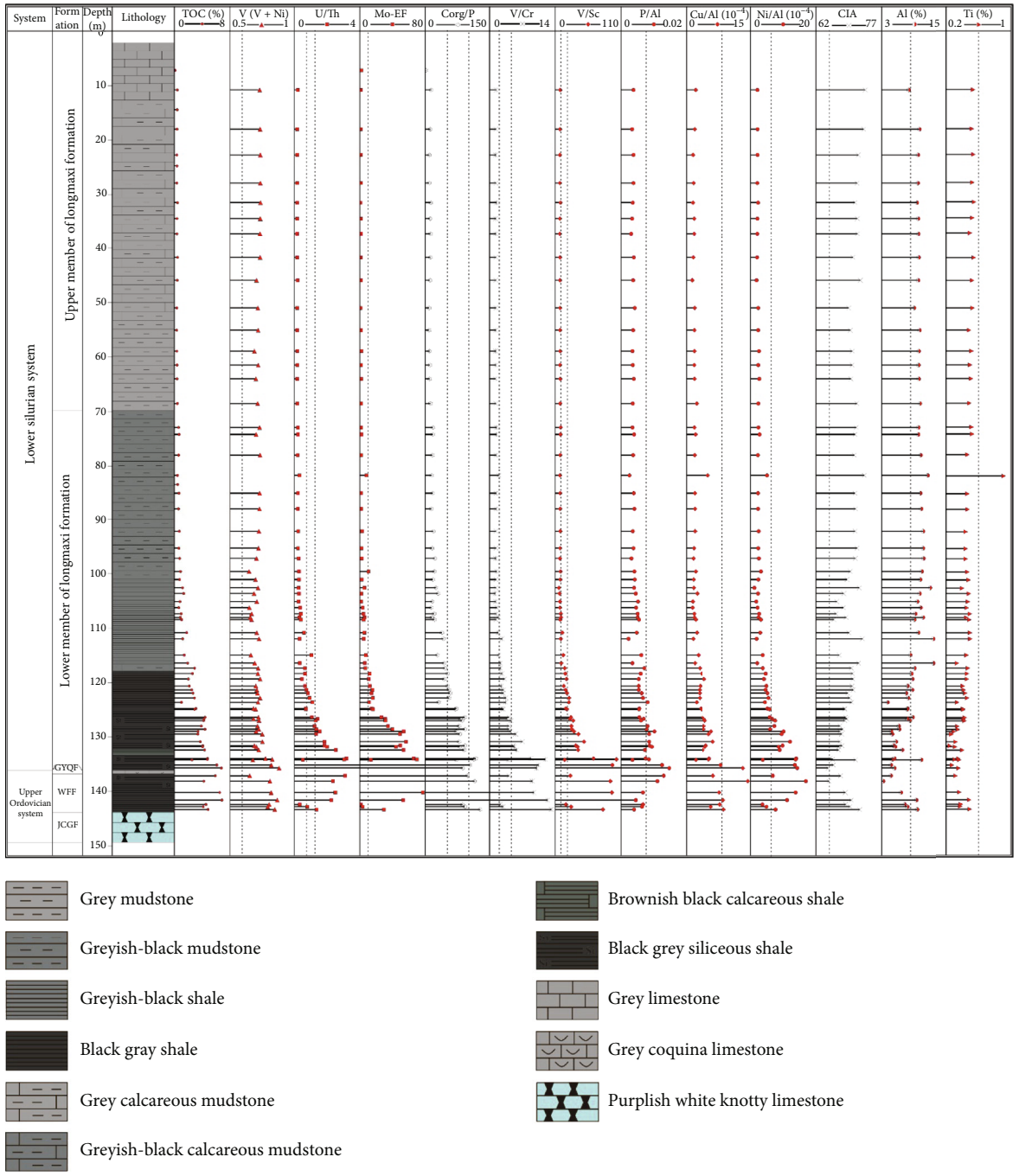

Figure 7: The vertical variations of the ratio of trace elements (reflecting redox condition and primary productivity) of studied samples and the ratio of major elements (CIA) (GYQF: Guanyinqiao Formation; WFF: Wufeng Formation; JCGF: Jiancaogou Formation).

the transfer of U from water column to sediments, resulting in uranium (U) enrichment in marine sediments [52]. The main sedimentary areas of authigenic U are anoxic basins, organic-rich continental shelves, and slope areas far away from the coast. The nickel (Ni) is occurred in the pyrite lattice in the form of insoluble nickel sulfide and preserved as Ni-porphyrin together with OM burial under a strong reduction environment [53]. Chromium (Cr) can be transformed from Cr^{4+} to Cr^{3+} under anoxic conditions and exported to sediments [24]. Molybdenum (Mo) is captured by iron (Fe) and manganese (Mn) oxides from water and sinks into sediments in an oxidizing environment [54, 55]. Under reducing conditions with low concentration of hydrogen sulfide, Mo is captured by Fe-S phase as active thiomolybdates. However, in the reduction condition of high hydrogen sulfide concentration, Mo is captured as a metal sulfide and precipitated in the absence of iron [54]. In addition, the preservation of organic carbon and organic phosphorus in marine sediments is controlled by the redox environment [56]. Eighty percent (80%) of total phosphorus comes from the organic matter [57]. Under reducing conditions, organic carbon is more conducive to preservation,

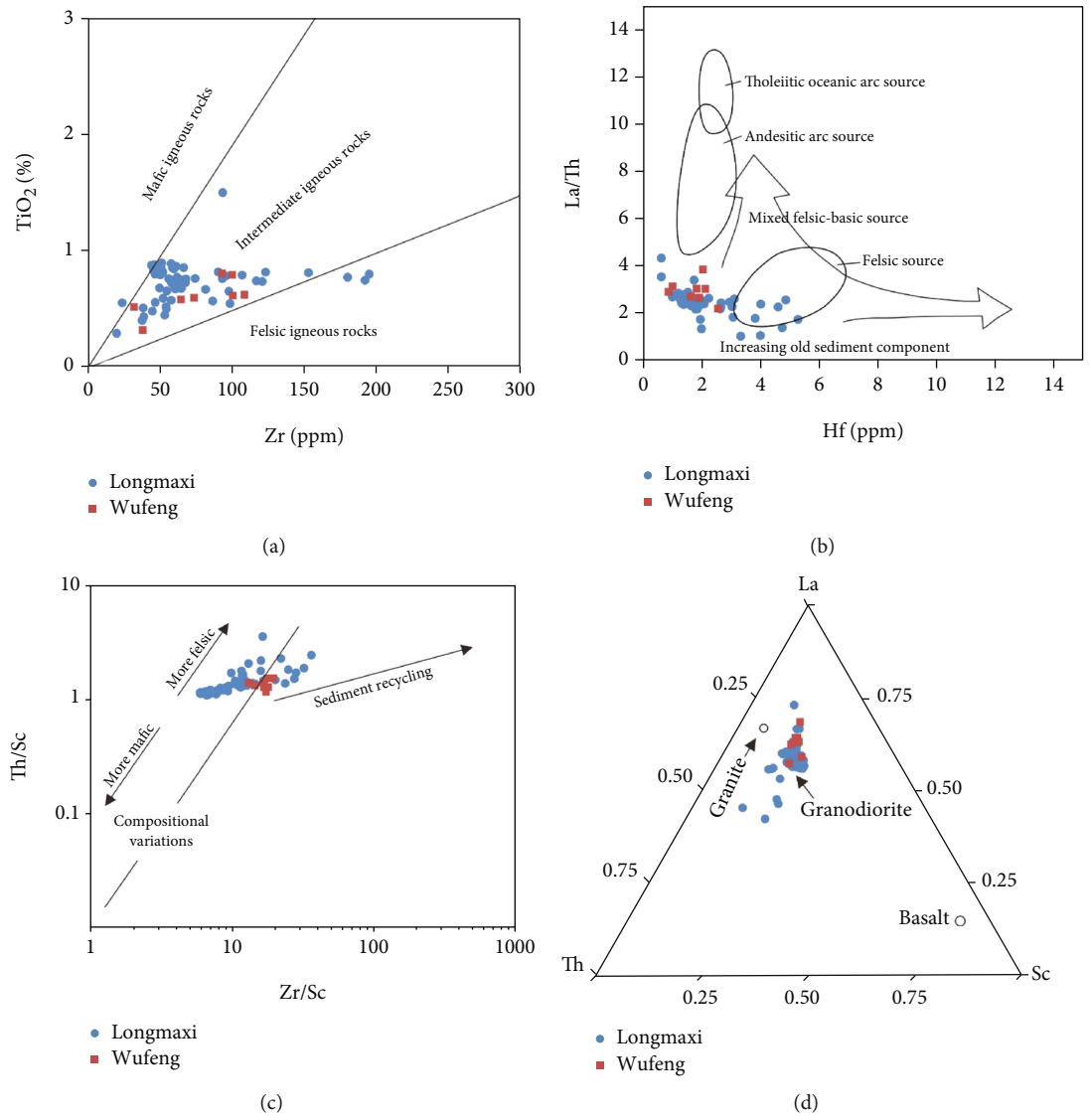

Figure 8: Diagrams for identifying the source of samples from Wufeng Formation and Longmaxi Formation [27–30].

while organic phosphorus content gradually decreases in the process of remineralization [56]. Therefore, C_{org}/P is used as an index to evaluate redox conditions [16, 58].

The ratios of these redox-sensitive trace elements (e.g., V/Cr, U/Th, V/(V + Ni), V/Sc, Mo_{EF}, and C_{org}/P) are used to trace redox changes in bottom water condition. The ratio of V/Cr as redox-sensitive index identifies the sedimentary environment. The V/Cr ratios are less than 2 and greater than 4.25, indicating oxic environment and anoxic (reducing) environment, respectively, and of 2 ~ 4.25 indicates the fluctuating redox conditions between oxic and anoxic bottom water conditions [59]. In this study, the V/Cr ratios of Wufeng Formation samples vary from 2.25 to 13.13 (avg. 7.9), indicating a strongly anoxic water condition, while the V/Cr ratios of Longmaxi Formation samples show an upward decreasing trend from 11.85 to 1.16, with an average of 2.76, indicating dominant anoxic water conditions with fluctuating dyoxic or oxic water conditions (Figure 7). The V/Sc and U/Th ratios greater than 20 and 1.25, respectively, indicate anoxic bottom water conditions, while V/Sc ratios of 9.1~20 and U/Th ratios of 0.75~1.25 generally suggest dysoxic conditions [60, 61]. However, the V/Sc and U/Th ratios less than 9.1 and 0.75, respectively, indicate that the sedimentary environment is closely related to oxic bottom water condition [60]. In this study, the values of V/Sc and U/Th for the Wufeng samples range from 17.99 to 175.99 (avg. 78.74) and 0.33 to 6.13 (avg. 2.35), respectively, indicating anoxic water condition. The same ratios of 5.08~102.33 (avg. 18.24) and 0.18~3.19 (avg. 0.74) for Longmaxi shales were as follows, suggesting dominant anoxic with fluctuating dyoxic or oxic water conditions (Figure 7). The V/(V + Ni) ratios of less than 0.60 are characteristics of both oxygenated and anoxic conditions [62]. The V/(V + Ni) ratios under anoxic and euxinic environments are 0.54~0.82 and greater than 0.82, respectively. The Longmaxi Formation samples show high V/(V + Ni) ratios of 0.44-0.82 (avg. 0.72), and its ratios vary from 0.66 to 0.88 (avg. 0.81) for Wufeng Formation samples (Figure 7). The ratios

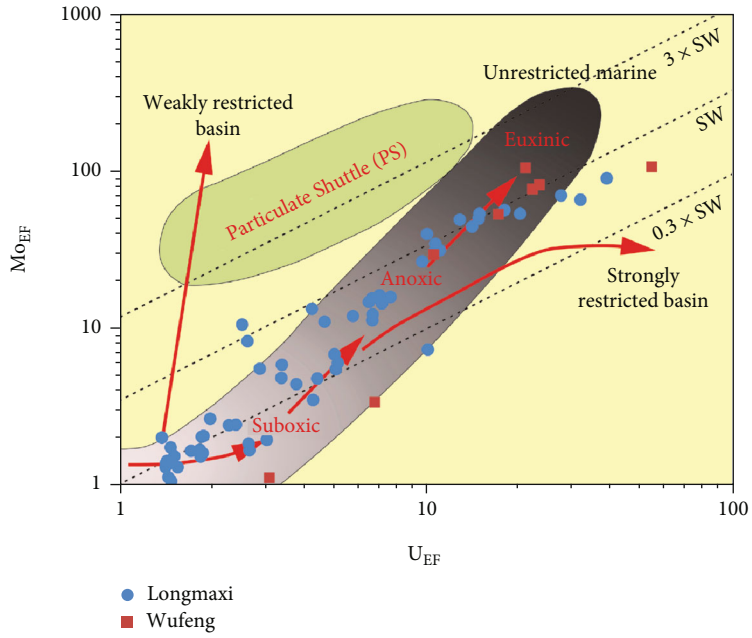

FIGURE 9: The covariation pattern of Mo_{EF} versus U_{EF} for the Wufeng Formation and Longmaxi Formation [16, 54, 55]. X_{EF} represents the enrichment factor of element X. The dotted lines are the multiples of Mo/U of modern seawater (0.3, 1, and 3).

indicate that the sedimentary environments for Wufeng and Longmaxi Formation shales are anoxic and intermittent euxinic bottom water conditions, which are also consistent with other redox proxies (Figure 7). The proxies discussed above are somewhat different due to different enrichment mechanisms of each trace element, but their indicative of the environment conditions and sedimentary characteristics is consistent [61].

In addition, molybdenum (Mo) was strongly enriched under anoxic and euxinic water conditions, showing $Mo_{EF} > 10$ but was moderately enriched under oxic water conditions, showing $Mo_{EF} < 10$ [54, 55]. In this study, the values of Mo_{EF} for the Wufeng samples and Longmaxi samples range from 1.13 to 106.26 (avg. 57.10) and 0.85 to 89.82 (avg. 15.05), respectively, indicating anoxic water condition. Because molybdenum and uranium exhibit differential enrichment under reducing conditions [54, 55], therefore, the combined conditions of molybdenum enrichment factor (Mo_{EF}) and U enrichment factor (U_{EF}) can be used to determine the redox conditions of Longmaxi Formation and Wufeng Formation. The covariation pattern of Mo_{EF} versus U_{EF} shows that both Wufeng Formation and Longmaxi Formation were deposited in unrestricted marine (Figure 9), while the Longmaxi Formation was mainly deposited in the dysoxic-anoxic-euxinic environment, and the ratio of Mo_{EF}/U_{EF} was 0.3, multiple of that of modern seawater to that of modern seawater. The Wufeng Formation was mainly deposited in the euxinic sedimentary environment, and the ratio of Mo_{EF}/U_{EF} was similar to that of modern seawater. The redox index $C_{org}/P < 50$ indicates that the sediment was deposited in an oxic environment, while $C_{org}/P > 100$ indicates that the sediment was deposited in an anoxic environment [57, 63]. The C_{org}/P ratios of Longmaxi Formation vary from 8.53 to 118.50 (avg. 40.28) and are lower than that of the Wufeng Formation shales (85.25 to 150.59, with an average of 114.57). This indicates that the bottom water environment from Wufeng Formation to Longmaxi Formation is from reduction to oxidation (Figure 7).

Obviously, according to the above redox proxies (V/Cr, U/Th, V/(V + Ni), V/Sc, Mo_{EF}, and C_{org}/P), the shales of the Wufeng Formation and Longmaxi Formation are deposited under reducing conditions. However, the reducibility decreased from Wufeng Formation to Longmaxi Formation. The sedimentary environment changed from euxinic to anoxic during the shale deposition from Wufeng Formation to the bottom of the lower Longmaxi Formation (Figure 7). In addition, from the top of the lower Longmaxi Formation to the upper Longmaxi Formation, the sedimentary environment changed from dysoxic to oxic (Figure 7).

5.3. The Coupled Relationship between TOC and Paleoproductivity Proxies. Paleomarine productivity provides high OM flux in the water column, which is finally preserved in marine sediments, contributing to OM accumulation. Although high flux of OM sink undergo the processes of mineralization and degradation in the water column, large amount of OM is still preserved in marine sediments owing to high marine productivity. The higher TOC contents in Wufeng shale (from 4.14% to 8.08%) may reflect high marine productivity in the surface waters and high level of OM flux, whereas the relatively low TOC contents in Longmaxi shale (0.09% to 4.76%) indicate decreasing marine productivity.

The phosphorus (P) is essential to living organisms, and its enrichment is closely related to biomass and organic

matter yield; so, it can be used as an indicator of productivity [15, 56]. A feedback loop between P recycling, anoxia of bottom water, and productivity of surface water may be linked [64]. The P/Al ratios of Longmaxi Formation vary from 0.0023 to 0.012 (avg. 0.0053) and are lower than that of the Wufeng Formation shales (0.0040 to 0.0147, with an average of 0.0084). There was a good match between the higher P/Al values and the higher TOC values in the Wufeng samples, which may indicate that partial P entered the sediment by adsorption to OM particles or coprecipitation in the form of authigenic phases owing to high productivity. The P/Al ratio of Wufeng Formation shales is mostly higher than those of average Post-Archean Australian Shale (PAAS), whereas these ratios from Longmaxi Formation are slightly lower than those of PAAS (0.0078, Figure 7) [65]. The above discussion indicates that the Longmaxi Formation samples were deposited in an environment of moderate to low paleoproductivity, and the Wufeng Formation samples were deposited in a high paleoproductivity environment. Generally, the Longmaxi shale implies relatively lower palaeoproductivity than those from Wufeng Formation shale. Interestingly, the changes in P/Al ratios of studied shales are coupled with the changes in TOC contents, further suggesting that the productivity may be a controlling factor for OM enrichment.

Other trace elements (e.g., Ni and Cu) are also bioessential elements and can be also used to describe paleoproductivity [15, 66]. These elements are transferred from surface water to the seafloor by absorption onto OM particles through microbial action and are mainly associated with pyrite and trapped in sediments after OM decay [24, 65, 67]. Particularly, the copper (Cu) is a good indicator of OM flux (productivity). The ratios of Cu/Al and Ni/Al for Longmaxi Formation range from 1.28×10^{-4} to 8.19×10^{-4} (avg. 2.85×10^{-4}) and 1.23×10^{-4} to 13.96×10^{-4} (avg. 4.48×10^{-4}), respectively, and such ratios for Wufeng shales are 5.93×10^{-4}~14.42×10^{-4} (avg. 9.19×10^{-4}) and 3.67×10^{-4}~16.91×10^{-4} (avg. 9.91×10^{-4}). The Cu/Al and Ni/Al ratios of Wufeng Formation shales are mostly higher than those of PAAS (8.93×10^{-4} and 7.14×10^{-4}), whereas these ratios from Longmaxi Formation are slightly lower than those of PAAS (8.93×10^{-4} and 7.14×10^{-4}). The high paleoproductivity levels in the Wufeng Formation may have been due to intense volcanic eruptions [68, 69] or to seasonal upwelling providing abundant nutrients [2, 70]. In conclusion, all the productivity proxy (P/Al, Cu/Al, and Ni/Al) ratios firstly show an increasing trend in Wufeng Formation samples, but they then begin to decrease in Longmaxi Formation samples. Their trend is also consistent with TOC contents, indicating relatively high productivity during the deposition of Wufeng Formation but moderate-low paleoproductivity during the deposition of Longmaxi Formation. Our results reveal that the OM enrichment is closely related to marine paleoproductivity in this study.

5.4. Controlling Factors for OM Enrichment. TOC contents of Wufeng and Longmaxi shales from XK1 are evidently different, which are 4.14%~8.08% (avg. 5.46%) and 0.09%~4.76% (avg. 1.79%), respectively. Generally, high TOC contents represent high OM enrichment. Hence, it is necessary to investigate the enrichment mechanism of OM.

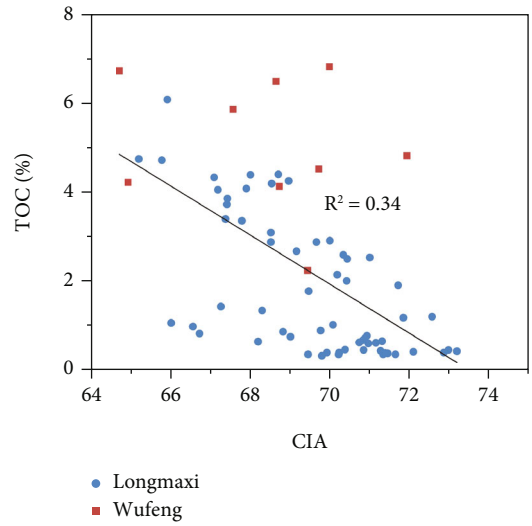

Figure 10: Correlations of geochemical parameter indicative of the paleoclimate and the TOC content.

During the deposition of shales, paleoclimate influenced the degree of provenance weathering and input of weathering nutrient, further playing a significant role in the OM abundance. According to CIA values, the climate of Upper Ordovician Wufeng Formation and Lower Silurian Longmaxi Formation is typically warm and humid with enhanced physical and chemical weathering. However, the CIA values present negative relationship with TOC content with relatively low correlation coefficient (Figure 10), indicating that the paleoclimate has a weak influence on OM enrichment but not the main factor for primary productivity. The contents of Al and Ti show moderate terrigenous input in Longmaxi Formation and lower terrigenous input in the Wufeng Formation. In addition, the negative correlation between the terrigenous input proxies (Al and Ti) and TOC (Figure 7) indicates that terrigenous detrital has a weak effect on organic matter accumulation, which is similar to the results of previous studies [16]. The TOC content is high, and terrigenous input is low in the Wufeng Formation and the bottom of upper Longmaxi Formation. This may be because less nutrients were brought by terrigenous inputs, but large amounts of nutrients were provided by volcanic activity [68, 69] or seasonal upwelling [2, 70] during this stage, resulting in higher productivity. The Upper Longmaxi Formation and the top of the lower Longmaxi Formation have stronger weathering and more terrigenous input (Figure 7). However, in the top of the lower Longmaxi Formation and the upper Longmaxi Formation, volcanic activity and upwelling were not developed, and nutrients were derived from terrestrial inputs; so, the productivity was lower than that of the Wufeng Formation and the bottom of the Upper Longmaxi Formation.

The productivity proxies P/Al (avg. 0.0053), Cu/Al (avg. 2.85×10^{-4}), and Ni/Al (avg. 4.48×10^{-4}) for the Longmaxi

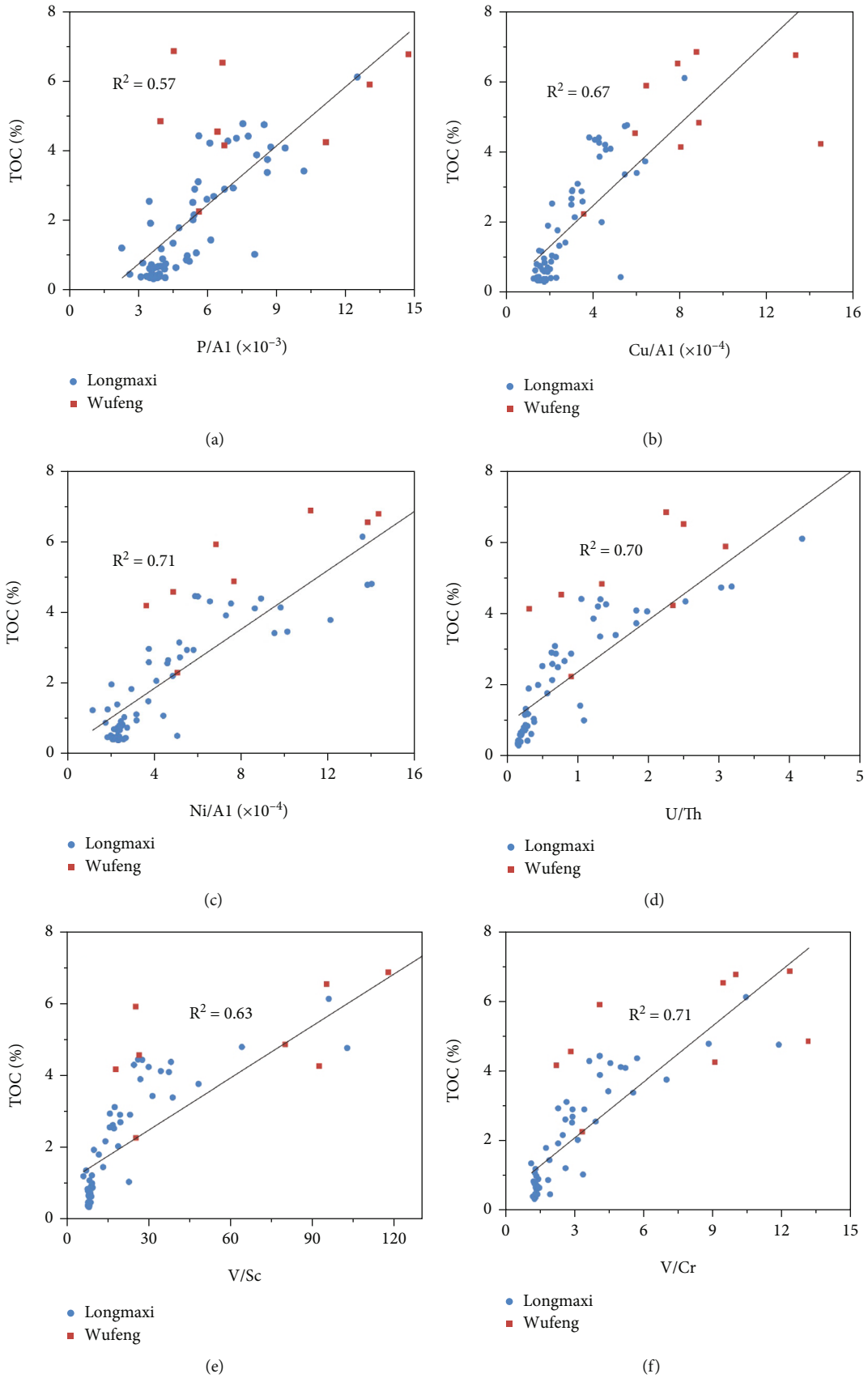

Figure 11: Correlations of geochemical indicative of the paleoproductivity, paleoredox, and TOC content.

Formation indicate moderate to relatively low paleoproductivity during the Longmaxi shale deposition. And such ratio average for the Wufeng Formation is 0.0084,9.19×10^{-4}, and9.91×10^{-4}, indicating high paleoproductivity during the Wufeng shale deposition. The moderate productivity may promote high OM flux in the water column that then is transferred into marine sediments. The relationships between TOC and P/Al, Cu/Al, and Ni/Al are positive with high correlation coefficients (R^2) of 0.57, 0.67, and 0.72, respectively (Figures 11(a)–11(c)), indicating that the paleoproductivity has an important influence on OM enrichment.

Redox conditions are another critical factors for controlling OM preservation. The ratios of redox-sensitive trace elements indicate that the studied samples from XK1 well were deposited under anoxic and dysoxic water conditions for Wufeng Formation and Longmaxi Formation. The paleoredox proxies (U/Th, V/Sc, and V/Cr) show positive correlation with TOC content with high correlation coefficients (0.70, 0.77, and 0.63, respectively) (Figures 11(d)–11(f)), indicating that the paleoredox conditions play an important role in OM accumulation. The Wufeng Formation shales have relatively high TOC contents, which are corresponding to anoxic water conditions, suggesting high efficient preservation of OM under anoxic conditions.

6. Conclusions

(1) The mineral compositions of the studied samples are quartz, clay minerals, calcite, and feldspar as well as minor dolomite, pyrite, and anhydrite. The source rocks are derived from acid-intermediate igneous rocks, and the representative mineral is granodiorite. In this study, the CIA values are in the main range of 65~85 for the Wufeng and Longmaxi Formations samples, indicating a typical warm and humid climate with enhanced physical and chemical weathering

(2) In conclusion, all the productivity proxy (P/Al, Cu/Al, and Ni/Al) ratios indicate that the paleoproductivity shows an upward decreasing trend from the Wufeng Formation to the Longmaxi Formation shales, which are also consistent with changes in TOC content. The productivity proxies indicate that the Wufeng Formation samples were deposited in relatively high paleoproductivity environment, Longmaxi Formation samples were deposited in moderate-low paleoproductivity environment, and productivity of the Wufeng Formation shales was higher than that of Longmaxi Formation shales

(3) The V/Cr ratios for the Wufeng and Longmaxi samples fluctuate from 2.25 to 13.13 (avg. 7.9) and 1.16 to 11.85 (avg. 2.76), respectively. The V/Sc and U/Th ratios of the Wufeng Formation samples range from 17.99 to 175.99 (avg. 78.74) and 0.33 to 6.13 (avg. 2.35), respectively, and the corresponding ratios for Longmaxi shales are from 5.08 to 102.33 (avg. 18.24) and from 0.18 to 3.19 (avg. 0.74), respectively. The values of Mo_{EF} for the Wufeng samples and Longmaxi samples range from 1.13 to 106.26 (avg. 57.10) and 0.85 to 89.82 (avg. 15.05), respectively. The C_{org}/P ratios of the Longmaxi Formation and Wufeng Formation shales vary from 8.53 to 118.50 (avg. 40.28) and 85.25 to 150.59 (avg. 114.57), respectively. These paleoredox proxies indicate that the oceanic environment conditions changed from anoxic of Wufeng Formation to dysoxic (oxic) of Longmaxi Formation

(4) The paleoclimate proxies present a negative relationship with TOC content with relatively low correlation coefficient. There is a positive correlation between productivity proxies and TOC content, and correlation coefficients are high. The paleoredox conditions have similar distribution trends and positive correlation with TOC content with high correlation coefficients. The above results indicate that OM enrichment for the Wufeng and Longmaxi shales is controlled by high productivity and anoxic bottom water conditions

Data Availability

The trace elements and rare earth data to this article are present in the supplementary material (Table S1).

Conflicts of Interest

The authors declare that they have no conflicts of interest.

Acknowledgments

This work was supported by the National Natural Science Foundation of China (Grant Nos. 41972155 and 41402130) and Gansu Science and Technology Program (22JR5RA045).

Supplementary Materials

The trace elements and rare earth data to this article are present in the supplementary material (Table S1). *(Supplementary Materials)*

References

[1] G. Chen, Y. Huang, and J. Li, *Geology Research Progress of Shale Gas in China*, Petroleum Industry Press, Beijing, China, 2011.

[2] Y. Lu, S. Jiang, Y. Lu, S. Xu, Y. Shu, and Y. Wang, "Productivity or preservation? The factors controlling the organic matter accumulation in the late Katian through Hirnantian Wufeng organic-rich shale, South China," *Marine and Petroleum Geology*, vol. 109, pp. 22–35, 2019.

[3] S. Yang, G. Chen, C. Lv et al., "Evolution of nanopore structure in lacustrine organic-rich shales during thermal maturation from hydrous pyrolysis, Minhe Basin, Northwest China," *Energy Exploration and Exploitation*, vol. 36, no. 2, pp. 265–281, 2018.

[4] Y. Li, S. Q. Pan, S. Z. Ning, L. Y. Shao, Z. H. Jing, and Z. S. Wang, "Coal measure metallogeny: metallogenic system and

implication for resource and environment," *Science China Earth Sciences*, vol. 65, no. 7, pp. 1211–1228, 2022.

[5] Y. Li and J. Chen, "Nanoscale mechanical property variations concerning mineral composition and contact of marine shale," *Geoscience Frontiers*, vol. 13, no. 4, article 101405, 2022.

[6] Y. Li and J. Chen, "Determination of shale macroscale modulus based on microscale measurement: a case study concerning multiscale mechanical characteristics," *Petroleum Science*, vol. 19, no. 3, pp. 1262–1275, 2022.

[7] Y. Yang, J. Zhang, X. Wang et al., "Source rock evaluation of continental shale gas: a case study of Chang 7 of Mesozic Yanchang Formation in Xia Siwan area of Yanchang," *Journal of Northeast Petroleum University*, vol. 36, no. 4, pp. 10–17, 2012.

[8] Q. S. Zhou, D. W. Zhang, X. T. Li et al., "Insight into the desorption behavior and mechanism of tight oil with in-situ low-temperature thermal," *Journal of Petroleum Science and Engineering*, vol. 218, article 111001, 2022.

[9] X. Wu, "Potential, distribution and key exploration fields," *Earth Science Frontiers*, vol. 29, no. 6, 2022.

[10] Y. Li, Z. Wang, Z. Pan, X. Niu, Y. Yu, and S. Meng, "Pore structure and its fractal dimensions of transitional shale: a cross-section from east margin of the Ordos Basin, China," *Fuel*, vol. 241, pp. 417–431, 2019.

[11] D. Dong, K. Cheng, Y. Wang, X. Li, S. Wang, and J. Huang, "Forming conditions sand characteristics of shale gas in the Lower Paleozoic of the Upper Yangtze region, China," *Oil Gas Geology*, vol. 31, no. 3, pp. 288–300, 2010.

[12] L. Wang, C. Zou, P. Zheng et al., "Geochemical evidence of shale gas existed in the Lower Paleozoie Sichuan basin," *Natural Gas Industry*, vol. 29, no. 5, pp. 59–62, 2009.

[13] S. Wang, L. Wang, J. Huang, X. Li, and D. Li, "Accumulation conditions of shale gas reservoirs in Siurian of the upper Yangtze region," *Natural Gas Industry*, vol. 29, no. 5, pp. 45–50, 2009.

[14] C. Zhang, W. Zhang, and Y. Guo, "Sedimentary environment and its effect on hydrocarbon source rocks of Longmaxi Formation in Southeast Sichuan and northern Guizhou," *Earth Science Frontiers*, vol. 19, no. 1, pp. 137–143, 2012.

[15] L. Tang, Y. Song, S. Jiang, Z. Jiang, and L. Xiao, "Organic matter accumulation of the Wufeng-Longmaxi shales in southern Sichuan Basin: evidence and insight from volcanism," *Marine & Petroleum Geology*, vol. 120, article 104564, 2020.

[16] C. Wei, T. Dong, Z. L. He et al., "Major, trace-elemental and sedimentological characterization of the Upper Ordovician Wufeng-Lower Silurian Longmaxi formations, Sichuan Basin, South China: insights into the effect of relative sea-level fluctuations on organic matter accumulation in shales," *Marine and Petroleum Geology*, vol. 126, article 104905, 2021.

[17] B. Xiao, S. G. Liu, Z. W. Li et al., "Geochemical characteristics of marine shale in the Wufeng Formation-Longmaxi Formation in the northern Sichuan Basin, South China and its implications for depositional controls on organic matter," *Journal of Petroleum Science and Engineering*, vol. 203, article 108618, 2021.

[18] C. N. Yan, Z. J. Jin, J. H. Zhao, W. Du, and Q. Y. Liu, "Influence of sedimentary environment on organic matter enrichment in shale: a case study of the Wufeng and Longmaxi formations of the Sichuan Basin, China," *Marine and Petroleum Geology*, vol. 92, pp. 880–894, 2018.

[19] C. Y. Wang, Z. T. Dong, X. H. Fu, X. Hu, and Z. Li, "Origin and paleoenvironment of organic matter in the Wufeng–Longmaxi shales in the northeastern Sichuan Basin," *Energy Exploration & Exploitation*, vol. 39, no. 4, 2020.

[20] M. Li and Y. Xie, "Sedimentary geochemistry characteristics and its sedimetary environment significance," *Inner Mongolia Petrochemical*, vol. 16, 2010.

[21] H. Sies, C. Berndt, and D. P. Jones, "Oxidative stress," *Annual Review of Biochemistry*, vol. 86, no. 1, pp. 715–748, 2017.

[22] R. Francois, "A study on the regulation of the concentrations of some trace metals (Rb, Sr, Zn, Pb, Cu, V, Cr, Ni, Mn and Mo) in Saanich Inlet Sediments, British Columbia, Canada," *Marine Geology*, vol. 83, no. 1-4, pp. 285–308, 1988.

[23] A. D. Russell and J. L. Morford, "The behavior of redox-sensitive metals across a laminated-massive-laminated transition in Saanich Inlet, British Columbia," *Marine Geology*, vol. 174, no. 1-4, pp. 341–354, 2001.

[24] N. Tribovillard, T. J. Algeo, T. Lyons, and A. Riboulleau, "Trace metals as paleoredox and paleoproductivity proxies: an update," *Chemical Geology*, vol. 232, no. 1-2, pp. 12–32, 2006.

[25] S. R. Taylor and S. M. McLennan, "The continental crust: its composition and evolution," *The Journal of Geology*, vol. 94, pp. 57–72, 1985.

[26] H. W. Nesbitt and G. M. Young, "Early Proterozoic climates and plate motions inferred from major element chemistry of lutites," *Nature*, vol. 299, no. 5885, pp. 715–717, 1982.

[27] P. Floyd and B. Leveridge, "Tectonic environment of the Devonian Gramscatho basin, South Cornwall: framework mode and geochemical evidence from turbiditic sandstones," *Journal of the Geological Society*, vol. 144, no. 4, pp. 531–542, 1987.

[28] K. I. Hayashi, H. Fujisawa, H. D. Holland, and H. Ohmoto, "Geochemistry of ~1.9 Ga sedimentary rocks from northeastern Labrador, Canada," *Geochimica et Cosmochimica Acta*, vol. 61, no. 19, pp. 4115–4137, 1997.

[29] A. V. Moradi, A. Sari, and P. Akkaya, "Geochemistry of the Miocene oil shale (Hançili Formation) in the Çankırı-Çorum Basin, Central Turkey: implications for Paleoclimate conditions, source-area weathering, provenance and tectonic setting," *Sedimentary Geology*, vol. 341, pp. 289–303, 2016.

[30] L. Zhai, C. Wu, Y. Ye, S. Zhang, and Y. Wang, "Fluctuations in chemical weathering on the Yangtze Block during the Ediacaran- Cambrian transition: implications for paleoclimatic conditions and the marine carbon cycle," *Palaeogeography, Palaeoclimatology, Palaeoecology*, vol. 490, pp. 280–292, 2018.

[31] C. N. Zou, Z. Yang, J. X. Dai et al., "The characteristics and significance of conventional and unconventional Sinian-Silurian gas systems in the Sichuan Basin, central China," *Marine and Petroleum Geology*, vol. 64, pp. 386–402, 2015.

[32] Z. Jin and L. Cai, "Inheritance and innovation of marine petroleum geological theory in China," *Acta Geologica Sinica*, vol. 17, no. 4, pp. 48–55, 2007.

[33] C. B. Shen, L. F. Mei, Z. P. Xu, and J. G. Tang, "Architecture and tectonic evolution of composite basin-mountain system in Sichuan basin and its adjacent areas," *Geotectonica Et Metallogenia*, vol. 31, no. 3, pp. 288–299, 2007.

[34] S. Liu, B. Deng, Y. Zhong, B. Ran, and Y. Ye, "Unique geological features of burial and superimposition of the Lower Paleozoic shale gas across the Sichuan Basin and its periphery," *Earth Science Frontiers*, vol. 23, no. 1, pp. 11–28, 2016.

[35] T. Pan, L. Zhu, Y. Wang, and X. M. Li, "Organic matter characteristics in Longmaxi Formation shale and their impacts on

shale gas enrichment in southern Sichuan," *Geological Journal of China Universities*, vol. 22, no. 2, pp. 344–349, 2016.

[36] G. Y. Zhu, S. C. Zhang, Y. B. Liang et al., "The characteristics of natural gas in Sichuan Basin and its sources," *Earth Science Frontiers*, vol. 13, no. 2, pp. 234–248, 2006.

[37] C. H. Cao, *Gas Geochemistry and Implication during Shale Gas Production of Longmaxi Formation in Sichuan Basin*, Lanzhou University, China, 2017.

[38] P. Zhang, J. C. Zhang, Y. Q. Huang, X. Tang, Z. P. Wang, and J. J. Peng, "Characteristics and gas content evolution of Wufeng-Longmaxi Formation shale in Well Xiye-1," *Resources and Industries*, vol. 17, no. 4, pp. 48–55, 2015.

[39] A. K. Zhao, Q. Yu, Z. H. Lei et al., "Geological and microstructural characterization of the Wufeng-Longmaxi shale in the basin-orogen transitional belt of North Guizhou Province, China," *Journal of Nanoscience and Nanotechnology*, vol. 17, no. 9, pp. 6026–6038, 2017.

[40] C. L. Mou, X. Y. Ge, X. S. Xu, K. K. Zhou, W. Liang, and X. P. Wang, "Lithofacies palaeogeography of the Late Ordovician and its petroleum geological significance in Middle-Upper Yangtze Region," *Palaeogeography, Palaeoclimatology, Palaeoecology*, vol. 16, no. 4, pp. 427–440, 2014.

[41] P. Zhang, J. C. Zhang, H. Liu, Y. Q. Huang, and Y. N. Lü, "Accumulation conditions of shale gas from Lower Silurian Longmaxi Formation in Guizhou," *Journal of Central South University(Science and Technology)*, vol. 47, no. 9, pp. 3085–3092, 2016.

[42] T. S. Yi and D. Gao, "Characteristics and distribution pattern of shale gas reservoir in Longmaxi Formation in Guizhou Province," *Coal Geology and Exploration*, vol. 43, no. 3, pp. 22–32, 2015.

[43] D. Yang, S. G. Liu, Y. M. Shan et al., "Fracture characteristics of shale in Upper Ordovician-Lower Silurian in Xishui Area, southeast of Sichuan Basin, China," *Journal of Chengdu University of Technology (Science and Technology Edition)*, vol. 40, no. 5, pp. 543–553, 2013.

[44] L. Qi, W. C. Yu, Y. S. Du et al., "Paleoclimate evolution of the cryogenian tiesi'ao Formation-datangpo Formation in eastern Guizhou province: evidence from the chemical index of alteration," *Geological Science and Technology Information*, vol. 34, no. 6, pp. 47–57, 2015.

[45] G. G. Lash and D. R. Blood, "Organic matter accumulation, redox, and diagenetic history of the Marcellus Formation, southwestern Pennsylvania, Appalachian basin," *Marine and Petroleum Geology*, vol. 57, pp. 244–263, 2014.

[46] T. J. Nameroff, S. E. Calvert, and J. W. Murray, "Glacial-interglacial variability in the eastern tropical North Pacific oxygen minimum zone recorded by redox-sensitive trace metals," *Paleoceanography*, vol. 19, no. 1, pp. 1010–1029, 2004.

[47] G. N. Breit and R. B. Wanty, "Vanadium accumulation in carbonaceous rocks: a review of geochemical controls during deposition and diagenesis," *Chemical Geology*, vol. 91, no. 2, pp. 83–97, 1991.

[48] J. L. Morford and S. Emerson, "The geochemistry of redox sensitive trace metals in sediments," *Geochimica et Cosmochimica Acta*, vol. 63, no. 11-12, pp. 1735–1750, 1999.

[49] R. B. Wanty and M. B. Goldhaber, "Thermodynamics and kinetics of reactions involving vanadium in natural systems: accumulation of vanadium in sedimentary rocks," *Geochimica et Cosmochimica Acta*, vol. 56, no. 4, pp. 1471–1483, 1992.

[50] G. Chaillou, P. Anschutz, G. Lavaux, J. Schäfer, and G. Blanc, "The distribution of Mo, U, and cd in relation to major redox species in muddy sediments of the Bay of Biscay," *Marine Chemistry*, vol. 80, no. 1, pp. 41–59, 2002.

[51] J. McManus, W. M. Berelson, G. P. Klinkhammer, D. E. Hammond, and C. Holm, "Authigenic uranium: relationship to oxygen penetration depth and organic carbon rain," *Geochimica et Cosmochimica Acta*, vol. 69, no. 1, pp. 95–108, 2005.

[52] B. Sundby, P. Martinez, and C. Gobeil, "Comparative geochemistry of cadmium, rhenium, uranium, and molybdenum in continental margin sediments," *Geochimica et Cosmochimica Acta*, vol. 68, no. 11, pp. 2485–2493, 2004.

[53] J. W. Morse and G. W. Luther, "Chemical influences on trace metal-sulfide interactions in anoxic sediments," *Geochimica et Cosmochimica Acta*, vol. 63, no. 19-20, pp. 3373–3378, 1999.

[54] T. J. Algeo and N. Tribovillard, "Environmental analysis of paleoceanographic systems based on molybdenum- uranium covariation," *Chemical Geology*, vol. 268, no. 3-4, pp. 211–225, 2009.

[55] N. Tribovillard, T. J. Algeo, F. Baudin, and A. Riboulleau, "Analysis of marine environmental conditions based on molybdenum-uranium covariation-applications to Mesozoic paleoceanography," *Chemical Geology*, vol. 324, pp. 46–58, 2012.

[56] T. J. Algeo and E. Ingall, "Sedimentary C_{org}:P ratios, paleocean ventilation, and Phanerozoic atmospheric pO_2," *Palaeogeography, Palaeoclimatology, Palaeoecology*, vol. 256, no. 3-4, pp. 130–155, 2007.

[57] S. D. Schoepfer, J. Shen, H. Wei, R. V. Tyson, E. Ingall, and T. J. Algeo, "Total organic carbon, organic phosphorus, and biogenic barium fluxes as proxies for paleomarine productivity," *Earth-Science Reviews*, vol. 149, pp. 23–52, 2015.

[58] X. Fu, J. Wang, S. Zeng, X. Feng, D. Wang, and C. Song, "Continental weathering and palaeoclimatic changes through the onset of the Early Toarcian oceanic anoxic event in the Qiangtang Basin, eastern Tethys," *Palaeogeography, Palaeoclimatology, Palaeoecology*, vol. 487, pp. 241–250, 2017.

[59] B. Jones and D. A. C. Manning, "Comparison of geochemical indices used for the interpretation of palaeoredox conditions in ancient mudstones," *Chemical Geology*, vol. 111, no. 1-4, pp. 111–129, 1994.

[60] J. R. Hatch and J. S. Leventhal, "Relationship between inferred redox potential of the depositional environment and geochemistry of the Upper Pennsylvanian (Missourian) Stark Shale Member of the Dennis Limestone, Wabaunsee County, Kansas, USA," *Chemical Geology*, vol. 99, no. 1-3, pp. 65–82, 1992.

[61] D. Yan, S. Li, H. Fu et al., "Mineralogy and geochemistry of Lower Silurian black shales from the Yangtze platform, South China," *International Journal of Coal Geology*, vol. 237, article 103706, 2021.

[62] S. Dai, D. Ji, C. R. Ward et al., "Mississippian anthracites in Guangxi Province, southern China: petrological, mineralogical, and rare earth element evidence for high-temperature solutions," *International Journal of Coal Geology*, vol. 197, pp. 84–114, 2018.

[63] T. J. Algeo and C. Li, "Redox classification and calibration of redox thresholds in sedimentary systems," *Geochimica et Cosmochimica Acta*, vol. 287, pp. 8–26, 2020.

[64] B. Zhang, S. Yao, W. Hu, H. Ding, B. Liu, and Y. Ren, "Development of a high-productivity and anoxic-euxinic condition during the late Guadalupian in the Lower Yangtze region:

implications for the mid- Capitanian extinction event," *Palaeogeography, Palaeoclimatology, Palaeoecology*, vol. 531, article 108630, 2019.

[65] J. Zhao, Z. Jin, Z. Jin, Y. Geng, X. Wen, and C. Yan, "Applying sedimentary geochemical proxies for paleoenvironment interpretation of organic-rich shale deposition in the Sichuan Basin, China," *International Journal of Coal Geology*, vol. 163, pp. 52–71, 2016.

[66] M. Rijkenberg, H. De Baar, K. Bakker et al., ""PRISTINE", a new high volume sampler for ultraclean sampling of trace metals and isotopes," *Marine Chemistry*, vol. 177, pp. 501–509, 2015.

[67] H. J. Brumsack, "The trace metal content of recent organic carbon-rich sediments: implications for Cretaceous black shale formation," *Palaeogeography, Palaeoclimatology, Palaeoecology*, vol. 232, no. 2-4, pp. 344–361, 2006.

[68] L. Wu, Y. Lu, S. Jiang, X. Liu, and G. He, "Effects of volcanic activities in Ordovician Wufeng-Silurian Longmaxi period on organic-rich shale in the Upper Yangtze area, South China," *Petroleum Exploration and Development*, vol. 45, no. 5, pp. 862–872, 2018.

[69] K. Zhao, X. Du, Y. Lu, F. Hao, Z. Liu, and J. Jia, "Is volcanic ash responsible for the enrichment of organic carbon in shales? Quantitative characterization of organic-rich shale at the Ordovician-Silurian transition," *GSA Bulletin*, vol. 133, no. 3-4, pp. 837–848, 2021.

[70] C. Jin, Z. Liao, and Y. Tang, "Sea-level changes control organic matter accumulation in the Longmaxi shales of southeastern Chongqing, China," *Marine and Petroleum Geology*, vol. 119, article 104478, 2020.

[71] C. F. Lyu, Y. Zhang, C. Li et al., "Pore characterization of Upper Ordovician Wufeng Formation and Lower Silurian Longmaxi Formation shale gas reservoirs, Sichuan Basin, China," *Journal of Natural Gas Geoscience*, vol. 5, no. 6, pp. 327–340, 2020.

[72] S. Paikaray, S. Banerjee, and S. Mukherji, "Geochemistry of shales from the paleoproterozoic to neoproterozoic Vindhyan Supergroup: implications on provenance, tectonics and paleoweathering," *Asian Earth Science*, vol. 32, no. 1, pp. 34–48, 2008.

[73] J. Schieber, "A combined petrographical-geochemical provenance study of the Newland Formation, Mid-Proterozoic of Montana," *Geological Magazine*, vol. 129, no. 2, pp. 223–237, 1992.